An Analogue of the Laplace-Runge-Lenz Vector for Timelike Geodesics in Schwarzschild Spacetime

by

Jordan A. Fazio

A THESIS SUBMITTED IN PARTIAL FULFILLMENT OF
THE REQUIREMENTS FOR THE DEGREE OF

MASTER OF SCIENCE

in

The Faculty of Mathematics and Sciences

Department of Physics

BROCK UNIVERSITY
July 10, 2019

Abstract

In Schwarzschild spacetime, the timelike geodesics are the trajectories of free, massive particles, orbiting a singularity at the origin $r = 0$. In this work we derive four scalar first integrals of timelike geodesics in Schwarzschild spacetime. Two of the first integrals, corresponding to energy and angular momentum, are well-known. The other two first integrals, an angular quantity and a temporal quantity, are not as well-known.

Using the freedom to shift first integrals by a constant value we set a 'zero-point' for each of the four first integrals. By choosing a natural point on a non-circular trajectory such as a turning point or inertial point to set the zero-point value, the angular and temporal first integrals will correspond respectively to the angle and time of the chosen zero-point. We then take the Newtonian limit of the angular and temporal first integrals, and show that using a natural choice of zero-point they provide a generalization of the classical Laplace-Runge-Lenz (LRL) vector.

We then evaluate the angular first integral for each type of timelike geodesic in Schwarzschild spacetime. In most cases we are able to choose a turning or inertial point to set a zero-point. For an unbound or asymptotic trajectory which falls into the singularity of the metric at $r = 0$, however, we find that we must take a different point, such as the point where the trajectory crosses the horizon at $r = 2M$, which we call the 'horizon point.' For the case of a precessing elliptic orbit we find that the angular first integral is multi-valued, with the zero-point jumping each time the trajectory crosses an apoapsis.

It is found that the angular and temporal first integrals provide a relativistic generalization of the classical LRL vector, where we the first integrals correspond to a larger class of physically meaningful points compared to Newtonian orbits and where the LRL vector and angular and temporal first integrals may always correspond to the periapsis.

Contents

List of Tables

List of Figures

List of Symbols

ds	(Schwarzschild) line element.
M	Mass of singularity at origin $r = 0$.
τ	Proper time.
σ	Proper time derivative of t, i.e. $\frac{dt}{d\tau}$.
v	Proper time derivative of r, i.e. $\frac{dr}{d\tau}$.
ω	Proper time derivative of ϕ, i.e. $\frac{d\phi}{d\tau}$.
u	Four-velocity, $\frac{d}{d\tau}(t\partial_t + r\partial_r + \phi\partial_\phi)$.
$g(a, b)$	Metric as a function of two four-vectors a and b.
$\hat{L}$	Angular momentum per unit mass.
$\hat{E}$	Energy per unit mass.
Θ	Angular first integral.
T	Temporal first integral.
p^t, p^r, p^ϕ	Components of four-momentum, p, in the equatorial hypersurface.
e_t, e_r, e_ϕ	Orthonormal frame vectors for stationary observers.
E, $p^{\hat{r}}$, $p^{\hat{\phi}}$	Local energy, radial momentum, and ϕ-momentum measured by stationary observers.
$\hat{V}_{\text{eff}}$, $\hat{F}_{\text{eff}}$	Schwarzschild effective radial potential and force.
r_*	Turning point.
r^*	Inertial point
$\hat{V}_{\text{New}}$, $\hat{E}_{\text{New}}$	Newtonian effective radial potential and Newtonian energy.
u_+, u_-	Turning point of Newtonian radial velocity equation. $u_+ > u_-$.

$\text{sgn}(\cdot)$	Sign function (1 for positive argument, -1 for negative argument, 0 if argument is 0).
$\bar{L}$	$\frac{\hat{L}}{2M}$.
$\bar{E}$	$\hat{E} + 1$.
$Q(u)$	Radial velocity equation as a function of $u = \frac{2M}{r}$ with $\bar{L}^2$ factored out. i.e. $v^2 = \bar{L}^2 Q(u)$.
Δ	Discriminant of radial velocity equation.
Δ_0	Discriminant of derivative of radial velocity equation.

Chapter 1

Preliminaries

The Schwarzschild metric is given by

$$(ds)^2 = -\frac{r-2M}{r}(dt)^2 + \frac{r}{r-2M}(dr)^2 + r^2\sin^2\theta(d\phi)^2 + r^2(d\theta)^2 \tag{1.1}$$

(see, for example, reference [7] for background in relativity). Note that (r, θ, ϕ) are standard spherical coordinates where $0 \leq r < \infty$, $0 \leq \theta \leq \pi$, and $0 \leq \phi < 2\pi$. Every timelike geodesic lies in a spatial hypersurface of constant θ and so hereafter we will put $\theta = \frac{\pi}{2}$ without loss of generality. The corresponding equatorial metric is given by

$$(ds)^2 = -\frac{r-2M}{r}(dt)^2 + \frac{r}{r-2M}(dr)^2 + r^2(d\phi)^2. \tag{1.2}$$

It will be useful to define the notation

$$\sigma = \dot{t},\ v = \dot{r},\ \omega = \dot{\phi} \tag{1.3}$$

where dots denote proper time (τ) differentiation.

Consider a free massive particle in the equatorial hypersurface. Its four-velocity is given by

$$u = \sigma\partial_t + v\partial_r + \omega\partial_\phi,\ -1 = g(u,u) \tag{1.4}$$

obeying the timelike geodesic equation

$$\frac{du}{d\tau} = 0 \tag{1.5}$$

and where $g(a,b)$ is the metric of vectors $a = a^t\partial_t + a^r\partial_r + a^\theta\partial_\theta + a^\phi\partial_\phi$ and $b =$

$b^t\partial_t + b^r\partial_r + b^\theta\partial_\theta + b^\phi\partial_\phi$ defined by

$$g(a,b) = -\frac{r-2M}{r}(a^t)(b^t) + \frac{r}{r-2M}(a^r)(b^r) + r^2\sin^2\theta(a^\theta)(b^\theta) + r^2(a^\phi)(b^\phi). \quad (1.6)$$

The equations of motion for the four-velocity components in equatorial Schwarzschild spacetime consist of

$$\frac{r-2M}{r}\dot{\sigma} + \frac{2M}{r^2}\sigma v = 0 \quad (1.7a)$$

$$\frac{r}{r-2M}\dot{v} - \frac{M}{(r-2M)^2}v^2 + \frac{M}{r^2}\sigma^2 - r\omega^2 = 0 \quad (1.7b)$$

$$r^2\dot{\omega} + 2r\omega v = 0. \quad (1.7c)$$

These equations together with the proper time equation

$$1 = \frac{r-2M}{r}\sigma^2 - \frac{r}{r-2M}v^2 - r^2\omega^2 \quad (1.8)$$

and the notation defined in (1.3) comprise a coupled system of second order ODEs for $(t(\tau), r(\tau), \phi(\tau))$

$$\dot{\sigma} = -\frac{2M}{r(r-2M)}\sigma v \quad (1.9a)$$

$$\dot{v} = (r-3M)\omega^2 - \frac{M}{r^2} \quad (1.9b)$$

$$\dot{\omega} = -\frac{2\omega v}{r} \quad (1.9c)$$

with the constraint

$$v^2 = \left(\frac{r-2M}{r}\right)^2\sigma^2 - r(r-2M)\omega^2 - \frac{r-2M}{r}. \quad (1.10)$$

Each solution $(t(\tau), r(\tau), \phi(\tau))$ describes a timelike geodesic in Schwarzschild spacetime. It is well known that these equations can be integrated to obtain the geodesics explicitly (see [6]). This reference also includes a discussion of the orbit types classified by root structure.

Chandrasekhar [6] provides a classification of the orbits in Schwarzschild spacetime, where every case but one is split into "orbits of the first kind" and "orbits of the second kind." We use this classification here, where for us it is sufficient to know that orbits of the second kind are those orbits that fall into the singularity, except

in the final case we discuss, where all orbits are considered orbits of the first kind. All other orbits are orbits of the first kind. For a derivation of the first integrals in a general central potential, including a Newtonian gravitational potential with a $\frac{1}{r^3}$ perturbation, see [2]. We use similar methods to this paper for finding the first integrals of our system. For a quick derivation of a discontinuous generalization of the LRL vector in a central $V(r) \sim \frac{1}{r}$ potential see [8]. For a generalization of the LRL vector to Bertrand spacetimes, see [3]. For a paper which connects the multi-valued nature of the LRL vector in general relativity to perihelion precession and the bending of light, see [4].

Chapter 2

Scalar First Integrals

A first integral of the timelike geodesic equations (1.9) is a scalar function

$$I(\tau, t, r, \phi, \sigma, v, \omega) \tag{2.1}$$

that is constant with respect to proper time, τ, on every timelike geodesic. Specifically, from the geodesic equations (1.9), I satisfies

$$\begin{aligned} 0 = \frac{dI}{d\tau} =& I_\tau + I_t\sigma + I_r v + I_\phi \omega - I_\sigma \frac{2M\sigma v}{r(r-2M)} \\ &+ I_v((r-3M)\omega^2 - \frac{M}{r^2}) - I_\omega \frac{2\omega v}{r}. \end{aligned} \tag{2.2}$$

This is a linear first-order PDE which can be turned into a system of ODEs using the method of characteristics:

$$\frac{d\tau}{1} = \frac{dt}{\sigma} = \frac{dr}{v} = \frac{d\phi}{\omega} = -\frac{r(r-2M)d\sigma}{2M\sigma v} = \frac{dv}{(r-3M)\omega^2 - \frac{M}{r^2}} = -\frac{r d\omega}{2\omega v}. \tag{2.3}$$

The process of solving this ODE system is equivalent to integrating the geodesic equations (1.9). From this point of view, first integrals correspond to arbitrary constants of integration.

Mathematically, the ODEs (2.3) are a first-order dynamical system for $(t(\tau), r(\tau), \phi(\tau), \sigma(\tau), v(\tau), \omega(\tau))$. There are five degrees of freedom because the proper time equation (1.8) provides a constraint among the six variables. Hence, the system will have five functionally independent first integrals. Four of these will describe constants of motion that have no explicit dependence on τ.

Physically, the constants of motion will represent energy, angular momentum, and two additional quantities which we will now derive.

2.1 Derivation

The ODEs (2.3) can be arranged into a triangular system in which the ODEs can be solved successively. First, we integrate $\frac{dr}{v} = -\frac{rd\omega}{2\omega v}$, which yields the constant of motion

$$I_1 = \omega r^2. \tag{2.4}$$

Integrating $\frac{dr}{v} = -\frac{r(r-2M)d\sigma}{2M\sigma v}$ yields

$$I_2 = \frac{r-2M}{r}\sigma. \tag{2.5}$$

As will be shown in the next section, I_1 and I_2 respectively correspond to angular momentum and energy per unit mass. Integrating $\frac{dr}{v} = \frac{dv}{(r-3M)\omega^2 - \frac{M}{r^2}}$ gives the proper time equation (1.10) which can be rewritten in terms of the constants of motion I_1 and I_2, Yielding an equation for radial velocity

$$v^2 = I_2^2 - \frac{r-2M}{r^3}I_1^2 - \frac{r-2M}{r}. \tag{2.6}$$

Next, we use I_1 to rewrite $\frac{d\phi}{\omega}$ as $\frac{r^2 d\phi}{I_1}$. Integrating $\frac{dr}{v} = \frac{r^2 d\phi}{I_1}$ then yields the constant of motion

$$I_3 = \phi - I_1 \int \frac{dr}{r^2 v}. \tag{2.7}$$

Finally, we use I_2 to rewrite $\frac{dt}{\sigma}$ as $\frac{(r-2M)dt}{rI_2}$. Integrating $\frac{dr}{v} = \frac{(r-2M)dt}{rI_2}$ yields the constant of motion

$$I_4 = t - I_2 \int \frac{rdr}{(r-2M)v}. \tag{2.8}$$

In addition to the four constants of motion I_1, I_2, I_3, and I_4, there is a proper-time dependent first integral which can be found by integrating $\frac{dr}{v} = \frac{d\tau}{1}$. Making use of the radial velocity equation (2.6) yields the first integral

$$I_5 = \tau - \mathrm{sgn}(v) \int \frac{r^{\frac{3}{2}}dr}{\sqrt{(I_2^2-1)r^3 + 2Mr^2 - I_1^2 r + 2MI_1^2}}. \tag{2.9}$$

2.2 Normalization (Zero-Point Values)

An arbitrary constant can be added to any first integral. This freedon represents the choice of a zero-point value for the first integral. For the constants of motion I_1, I_2,

I_3, and I_4, we write

$$I_1 = \hat{L} + \hat{L}_0$$
$$I_2 = \hat{E} + \hat{E}_0$$
$$I_3 = \Theta + \Theta_0$$
$$I_4 = T + T_0$$

where $\hat{L}$, $\hat{E}$, Θ, and T denote the normalized constants of motion and $\hat{L}_0$, $\hat{E}_0$, Θ_0, and T_0 denote the zero-point constants. The remainder of this section will be dedicated to choosing physically meaningful zero-point constants for each of the constants of motion.

We first note that the four-momentum of a massive free particle in the equatorial hypersurface is given by

$$p = p^t \partial_t + p^r \partial_r + p^\phi \partial_\phi = mu \tag{2.10}$$
$$p^t = m\sigma,\ p^r = mv,\ p^\phi = m\omega \tag{2.11}$$

where m is the rest mass of the particle. The components of four-momentum have a natural physical meaning with respect to stationary observers in the equatorial hypersurface. An orthonormal frame for these observers is

$$e_t = \sqrt{\frac{r}{r-2M}}\partial_t, \quad e_r = \sqrt{\frac{r-2M}{r}}\partial_r, \quad e_\phi = \frac{1}{r}\partial_\phi. \tag{2.12}$$

Then the local energy, radial momentum, and ϕ-momentum measured by the stationary observers are respectively

$$E = -g(e_t, p) = \sqrt{\frac{r-2M}{r}}p^t \tag{2.13}$$
$$p^{\hat{r}} = g(e_r, p) = \sqrt{\frac{r}{r-2M}}p^r \tag{2.14}$$
$$p^{\hat{\phi}} = g(e_\phi, p) = rp^\phi. \tag{2.15}$$

We can use these expressions along with the components of momentum (2.11) to find physically meaningful values for $\hat{L}_0$, $\hat{E}_0$.

To find a physically meaningful choice for $\hat{L}_0$, we write $p^{\hat{\phi}}$ in terms of the first

integral $\hat{L} + \hat{L}_0$:

$$p^{\hat{\phi}} = \frac{m\omega r^2}{r} = \frac{m}{r}(\hat{L} + \hat{L}_0). \tag{2.16}$$

Rearranging yields

$$\hat{L} = \frac{rp^{\hat{\phi}}}{m} - \hat{L}_0, \tag{2.17}$$

which has units of angular momentum per unit mass. We want $\hat{L} = 0$ when $\omega = 0$. This implies $\hat{L}_0 = 0$. Then

$$\hat{L} = \frac{rp^{\hat{\phi}}}{m} = r^2\omega \tag{2.18}$$

is the angular momentum per unit mass.

Rewriting the local energy (2.13) in terms of $\hat{E} + \hat{E}_0$ yields

$$E = \sqrt{\frac{r-2M}{r}}m\sigma = m\sqrt{\frac{r}{r-2M}}(\hat{E} + \hat{E}_0). \tag{2.19}$$

Rearranging for $\hat{E}$ yields

$$\hat{E} = \sqrt{\frac{r-2M}{r}}\frac{E}{m} - \hat{E}_0. \tag{2.20}$$

Consider a particle at rest at radial infinity, so that $E = m$ and thus $\hat{E}|_{r=\infty} = 1 - \hat{E}_0$. We want either $\hat{E} = 0$, representing energy without a rest-mass contribution, or $\hat{E} = 1$, representing total mass-energy. These differ by a constant and so the choice amounts to making a convention. We will pick $\hat{E} = 0$, which gives $\hat{E}_0 = 1$. Then the constant of motion becomes

$$\hat{E} = \sqrt{\frac{r-2M}{r}}\frac{E}{m} - 1, \tag{2.21}$$

which physically describes the local energy per unit mass multiplied by a redshift factor (see ref. [7, 9]). This choice of zero-point has the advantage in the Newtonian limit, considered later, that $\hat{E}$ reduces to the Newtonian energy per unit mass.

Using the first integrals (2.18) and (2.21) we have so far, the radial velocity equation (2.6) becomes

$$v^2 = (\hat{E} + 1)^2 - \frac{r-2M}{r^3}\hat{L}^2 - \frac{r-2M}{r}. \tag{2.22}$$

Rearrange this equation to get

$$\hat{E} = \frac{1}{2}v^2 + \frac{r-2M}{2r^3}\hat{L}^2 + \frac{r-2M}{2r} - \frac{1}{2}(\hat{E}^2 + 1). \tag{2.23}$$

Ignoring the constant term, this yields the Schwarzschild effective potential per unit mass

$$\hat{V}_{\text{eff}} = \frac{r-2M}{2r^3}\hat{L}^2 + \frac{r-2M}{2r}. \tag{2.24}$$

The radial derivative of the effective potential gives the effective radial force per unit mass:

$$\hat{F}_{\text{eff}} = \frac{\partial \hat{V}_{\text{eff}}}{\partial r} = \frac{M}{r^2} - \frac{\hat{L}^2}{r^3} + \frac{3M\hat{L}^2}{r^4}. \tag{2.25}$$

We now explain a physically natural choice of zero-point in the angular and temporal first integrals (2.7) and (2.8). Using $\hat{L}$ and $\hat{E}$, the angular first integral (2.7) can be written

$$\Theta = \phi - \hat{L}\int \frac{dr}{r^2 v} - \Theta_0. \tag{2.26}$$

We can then absorb Θ_0 into a choice of integration constant r_0

$$\Theta = \phi - \hat{L}\int_{r_0}^{r} \frac{dr}{r^2 v}. \tag{2.27}$$

Similar to the angular first integral, we can write the temporal first integral (2.8) as

$$T = t - (\hat{E}+1)\int \frac{r dr}{(r-2M)v} - T_0 = t - (\hat{E}+1)\int_{r_0}^{r} \frac{r dr}{(r-2M)v}. \tag{2.28}$$

We choose r_0 in T to be the r_0 in Θ.

There are two dynamically natural choices for r_0:

1. A turning point, denoted r_*, which is defined as a point at which the radial velocity, v, is zero. Turning points are given by the positive real roots of the radial velocity equation (2.22)

$$(\hat{E}+1)^2 r_*^3 - (r_*-2M)r_*^2 - \hat{L}^2(r_*-2M) = 0. \tag{2.29}$$

2. An inertial point, denoted r^*, which is defined as a radial value where the effective radial force $\hat{F}_{\text{eff}}$ vanishes. From the radial force equation (2.25)

$$r^* = \frac{\hat{L}^2}{2M}\left[1 \pm (1 - 12\frac{M^2}{\hat{L}^2})^{\frac{1}{2}}\right]. \tag{2.30}$$

Additionally, for relativistic orbits that cross the event horizon at radial value $r = 2M$, we can define a horizon point as the point on the orbit with radial value $r_{\text{hor}} = 2M$.

Of the four constants of motion, the angular momentum $\hat{L}$ and energy per unit

mass $\hat{E}$ are well-known, while Θ and T are new. First, we explore Θ and T in the Newtonian limit so that we can compare our relativistic quantities to the simpler Newtonian ones. We will then use the well-known classification of orbits in the Schwarzschild metric (see [6] for example) to explore Θ and T. There is a particular interest in the physical meaning of each of these quantities.

Chapter 3

Newtonian Limit

In this section we evaluate the first integrals Θ and T in the Newtonian limit and show that Θ corresponds to the angle of the LRL vector with a suitable choice of zero-point value r_0.

Letting $r \gg 2M$ and keeping $\hat{L}$ finite, the effective potential per unit mass (2.24) becomes

$$\hat{V}_{\text{New}} = -\frac{GM}{r} + \frac{\hat{L}^2}{2r^2}, \tag{3.1}$$

which is the Newtonian potential per unit mass. The energy per unit mass (2.23) then becomes

$$\hat{E}_{\text{New}} = \frac{1}{2}v^2 + \hat{V}_{\text{New}}. \tag{3.2}$$

In the Newtonian limit, the temporal first integral (2.28) becomes

$$T \approx t - \int_{r_0}^{r} \frac{dr}{v}, \tag{3.3}$$

where

$$v^2 = 2\hat{E}_{New} - 2\hat{V}_{New} \tag{3.4}$$

is the Newtonian radial velocity. Note that (3.3) is equivalent to $v = \frac{dr}{dt}$. The angular first integral (2.27) remains unchanged apart from the change in radial velocity expression.

In Newtonian gravity, the possible trajectories of massive particles are circular, elliptic, parabolic, and hyperbolic. For circular orbits r is constant and $v = 0$, so Θ and T are undefined. We will thus consider only non-circular orbits. For elliptic orbits $\hat{E}_{New} < 0$, while for parabolic orbits $\hat{E}_{New} = 0$, and for hyperbolic orbits $\hat{E}_{New} > 0$. To find explicit closed-form expressions for Θ and T, we start by substituting $u = \frac{1}{r}$

in the Newtonian radial velocity expression (3.4), which we write as

$$v^2 = -\hat{L}^2(u - u_-)(u - u_+). \tag{3.5}$$

The positive real roots of this equation correspond to physical turning points on the trajectory. For elliptic orbits we have two turning points corresponding to two positive real roots, while for parabolic and hyperbolic orbits we have only one turning point, corresponding to a single positive real root. In all cases, we need both roots of equation (3.5) for evaluating the quadrature.

The roots are given by

$$u_- = \frac{M}{\hat{L}^2}\left(1 - \sqrt{1 + \frac{2\hat{E}_{New}\hat{L}^2}{M^2}}\right) \tag{3.6}$$

$$u_+ = \frac{M}{\hat{L}^2}\left(1 + \sqrt{1 + \frac{2\hat{E}_{New}\hat{L}^2}{M^2}}\right), \tag{3.7}$$

where $u_+ > u_-$. We will evaluate the first integrals for each type of orbit separately.

For an elliptic orbit, $u_- > 0$ and the range of u is $u_- \leq u \leq u_+$. Evaluating the angular and temporal first integrals (2.27) and (3.3) for an elliptic orbit yields

$$\Theta = \phi + 2\mathrm{sgn}(v\hat{L}) \arctan \sqrt{\frac{u - u_-}{u_+ - u}}\Bigg|_{u_0}^{u} \tag{3.8}$$

$$T = t + \frac{\mathrm{sgn}(v)}{2\hat{L}\sqrt{u_-u_+}}\Bigg[\Big(\frac{1}{u_-} + \frac{1}{u_+}\Big) \arctan \sqrt{\frac{u_+(u - u_-)}{u_-(u_+ - u)}} + \Big(\frac{1}{u_-} - \frac{1}{u_+}\Big)\frac{\sqrt{u_-u_+(u - u_-)(u_+ - u)}}{u_+(u - u_-) + u_-(u_+ - u)}\Bigg]\Bigg|_{u_0}^{u}. \tag{3.9}$$

Expression (3.8) for Θ will be valid for all types of orbits, but T will have to be evaluated in each case separately.

For a parabolic orbit, $u_- = 0$ and the range of u is $0 < u \leq u_+$. Evaluating the temporal first integral for a parabolic orbit yields

$$T = t - \frac{\mathrm{sgn}(v\hat{L})}{3\hat{L}u_+^2}\Big(2 + \frac{u_+}{u}\Big)\sqrt{\frac{u_+ - u}{u}}\Bigg|_{u_0}^{u}. \tag{3.10}$$

For a hyperbolic orbit, $u_- < 0$ and the range of u is $0 < u \leq u_+$. Evaluating the

temporal first integral for a hyperbolic orbit yields

$$T = t + \frac{\operatorname{sgn}(v)}{2\hat{L}\sqrt{|u_-|u_+}}\left[\left(\frac{1}{u_-}+\frac{1}{u_+}\right)\operatorname{arctanh}\sqrt{\frac{u_+(u-u_-)}{|u_-|(u_+-u)}}\right. \\ \left. -\left(\frac{1}{u_-}-\frac{1}{u_+}\right)\frac{\sqrt{|u_-|u_+(u-u_-)(u_+-u)}}{u_+(u-u_-)+u_-(u_+-u)}\right]\Bigg|_{u_0}^{u}. \tag{3.11}$$

By choosing $u_0 = \frac{1}{\min(r_*)}$, which corresponds to the smallest turning point on an elliptic orbit or the only turning point on a parabolic or hyperbolic orbit, Θ and T correspond respectively to the angle and time on the orbit with the smallest radial value. This point is called the *periapsis* point. The first integrals Θ and T when normalized in this way are analogous to the Laplace-Runge-Lenz vector, which is a conserved vector quantity that points from the origin to the direction of the periapsis point.

Chapter 4

LRL Angle for Schwarzschild Orbits

We now carry out a similar analysis of Θ and T for the Schwarzschild spacetime. It will be convenient to let

$$u = \frac{2M}{r} \tag{4.1a}$$

$$\bar{L} = \frac{\hat{L}}{2M} \tag{4.1b}$$

$$\bar{E} = \hat{E} + 1. \tag{4.1c}$$

This yields radial velocity equation (2.22) as a cubic polynomial in u:

$$v^2 = \bar{L}^2 Q(u), \quad Q(u) = u^3 - u^2 + \bar{L}^{-2}u + (\bar{E}^2 - 1)\bar{L}^{-2} \tag{4.2}$$

for which we can determine the root structure using Cardano's method (see ref. [5, 1]). Each positive root of this equation corresponds to a physical turning point on the orbit. It is now convenient to write the inertial point (2.30) with these substitutions:

$$u^* = \bar{L}^{-2}\left[1 \pm (1 - 3\bar{L}^{-2})^{\frac{1}{2}}\right]^{-1}. \tag{4.3}$$

We substitute (4.2) in the angular first integral (2.27) and the temporal first

integral (2.28):

$$\Theta = \phi + \int_{u_0}^{u} \frac{\operatorname{sgn}(v\bar{L})du}{\sqrt{Q(u)}} \tag{4.4}$$

$$T = t + \frac{2M\bar{E}}{|\bar{L}|} \int_{u_0}^{u} \frac{\operatorname{sgn}(v)du}{(1-u)u^2\sqrt{Q(u)}}. \tag{4.5}$$

Once we know the root structure of $Q(u)$ we can compute the above integrals. The root structure is determined by the discriminant Δ and another quantity denoted Δ_0 which are given by:

$$\Delta = 4(\bar{E}^2 - 1)\bar{L}^{-2} + \left(4 - 27\left(\bar{E}^2 - \frac{2}{3}\right)^2\right)\bar{L}^{-4} - 4\bar{L}^{-6} \tag{4.6a}$$

$$\Delta_0 = 1 - 3\bar{L}^{-2}. \tag{4.6b}$$

There are four possible root structures, each corresponding to specific classes of orbits. We may have either bound or unbound orbits, defined by $\bar{E}^2 < 1$ and $\bar{E}^2 \geq 1$ respectively. Each case except the case with a pair of complex conjugate roots has two distinct orbits called orbits of the first and second kinds. Below is a brief description of the physical orbits in each root structure (for more detail, see [6]):

- Triple real root ($\Delta = 0$, $\Delta_0 = 0$): the orbits of the first kind are unstable circular orbits at r_1, the sole radial value where $v^2 = 0$. The orbits of the second kind asymptotically spiral into the singularity from aphelion r_1.
- Double real root ($u_2 = \frac{2M}{r_2}$) and single real root ($u_1 = \frac{2M}{r_1}$) ($\Delta = 0$, $\Delta_0 \neq 0$):
  - When the double root is greater than the single root, the orbits of the first kind come in from radial value r_1 (finite for $\bar{E} < 1$, infinite otherwise) and asymptotically spiral in to a circle of radial value r_2. The orbits of the second kind fall into the singularity by asymptotically spiralling in from r_2.
  - When the single root is greater than the double root, the orbits of the first kind are stable circular orbits at r_2 and the orbits of the second kind fall into the singularity starting from radial value r_1.
- Three real roots ($u_1 < u_2 < u_3$, $u_i = \frac{2M}{r_i}$; $\Delta > 0$): depending on whether $\bar{E} < 1$, $\bar{E} = 1$, or $\bar{E} > 1$ the orbits of the first kind are the Schwarzschild analogues to the elliptic, parabolic, and hyperbolic orbits (respectively) from Newtonian gravity. There is a perihelion at r_2 and aphelion (for elliptic orbits)

at r_1. Unlike their Newtonian counterparts, these orbits may precess or loop around the singularity. The orbits of the second kind fall into the singularity from radial value r_3.

- One real root, two complex conjugate roots (u_1 real, $u_2 = \overline{u_3}$; $\Delta < 0$): all orbits fall into the singularity, either from aphelion r_1 or from infinity if $u_1 \leq 0$.

4.1 Triple Real Root

Figure 4.1: In the triple real root case the orbit of the first kind is an unstable circular orbit (red) and the orbit of the second kind asymptotic spiral (green). The horizon is drawn at $u = 1$ in black. For the asymptotic spiral, we can take the zero-point to be the horizon point, $u_0 = 1$, marked by a cross.

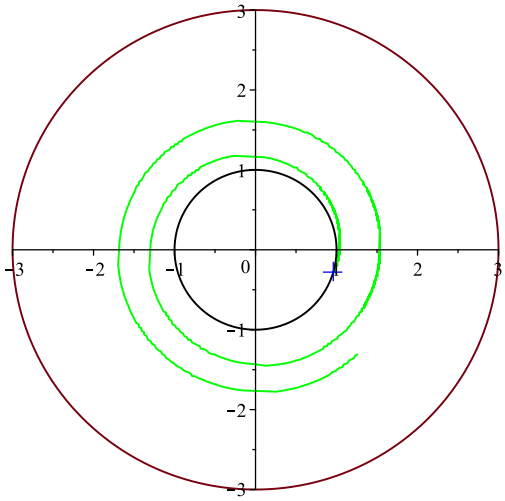

The triple real root structure is determined by the conditions

$$\Delta = 0 \tag{4.7a}$$

$$\Delta_0 = 0. \tag{4.7b}$$

These conditions yield

$$\bar{L}^{-2} = \frac{1}{3} \tag{4.8a}$$

$$\bar{E}^2 = \frac{8}{9}. \tag{4.8b}$$

$Q(u)$ then has a triple root:

$$u_1 = \frac{1}{3}. \tag{4.9}$$

Because $\bar{E}^2 = \frac{8}{9} < 1$ this case only contains bound orbits. There is an unstable circular orbit at $r_1 = \frac{2M}{u_1} = 6M$ and an orbit that falls into the singularity from r_1.

For the unstable circular orbit, (2.27) is not well-defined. For the falling in orbit, the first integral evaluates to:

$$\Theta = \phi - 2\,\mathrm{sgn}(v\bar{L})\left[\left(u - \frac{1}{3}\right)^{-\frac{1}{2}} - \left(u_0 - \frac{1}{3}\right)^{-\frac{1}{2}}\right]. \tag{4.10}$$

By using equation (4.3) we find that $u^* = \frac{1}{3}$. Since $u^* = u_1 = \frac{1}{3}$ gives a singular result in the first integral we are unable to choose u_0 to be an inertial or turning point. Instead, we choose u_0 to be the horizon point, where the spiral crosses the horizon at $r = 2M$.

4.2 Double Real Root and a Single Real Root

Figure 4.2: The bound (left) and unbound (right) orbits of the first kind when $u_2 > u_1$. The bound orbit of the first kind has apoapsis $r_1 = \frac{2M}{u_1}$ (solid dot). Both bound and unbound orbits of the first kind asymptotically spiral into $r_2 = \frac{2M}{u_2}$ (dashed). Inertial points are marked by diamonds. We can choose u_0 to correspond to the apoapsis (bound orbits only) or an inertial point.

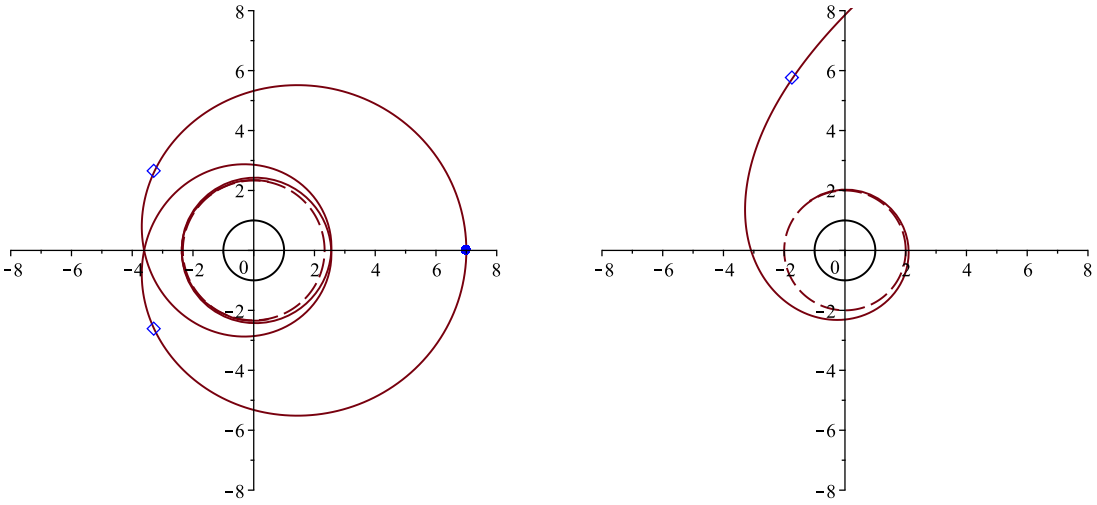

Figure 4.3: The orbit of the second kind asymptotically spirals into the singularity with asymptote $r_2 = \frac{2M}{u_2}$. We can choose u_0 to be the horizon point.

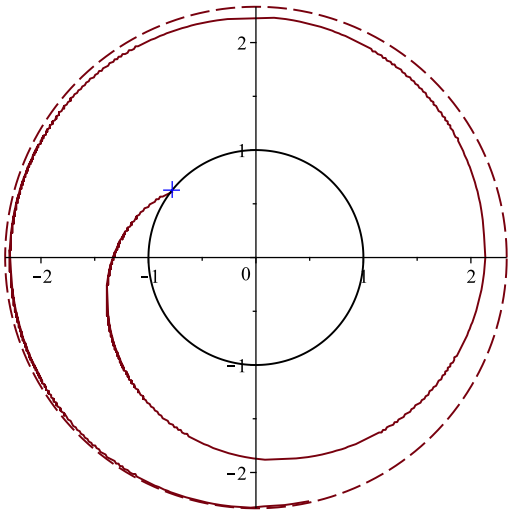

The root structure in this case is determined by the conditions

$$\Delta = 0 \tag{4.11a}$$

$$\Delta_0 \neq 0 \tag{4.11b}$$

which yield

$$\bar{L}^{-2} = \frac{1}{2} - \frac{27}{8}\Big[\big(\bar{E}^2 - \frac{2}{3}\big)^2 \pm |\bar{E}|\big(\bar{E}^2 - \frac{8}{9}\big)^{\frac{3}{2}}\Big] \neq \frac{1}{3}. \tag{4.12}$$

Then $Q(u)$ has a single root given by

$$u_1 = 1 - \frac{9\bar{E}^2 - 8}{1 - 3\bar{L}^{-2}}\bar{L}^{-2} \tag{4.13}$$

and a double root given by

$$u_2 = \frac{1}{2}\frac{9\bar{E}^2 - 8}{1 - 3\bar{L}^{-2}}\bar{L}^{-2}. \tag{4.14}$$

By analysis of (4.12), we see that $\bar{L}^{-2}$ is only positive for $\frac{8}{9} < \bar{E}^2 < 1$ when we take the plus sign and $\bar{E}^2 > \frac{8}{9}$ when we take the minus sign. Using (4.12) to eliminate $\bar{L}^{-2}$ in favour of $\bar{E}^2$ in the expressions for our roots we can determine which of u_1 and u_2 is larger, which will determine the shape of the orbits and the form of the first integrals. We find that which turning point is larger depends on which sign we take in (4.12). When we take the minus sign in (4.12):

- $\bar{E}^2 > \frac{8}{9}$

Figure 4.4: The orbits of the first and second kind for $u_1 > u_2$. The orbit of the first kind (red) is a stable circular orbit at r_2. The orbit of the second kind (green) falls into the singularity with apoapsis $r_1 = \frac{2M}{u_1}$. For the circular orbit of the first kind, the first integral is undefined. For the orbit of the second kind we can choose u_0 to correspond to the apoapsis ($u_0 = u_1$) or the horizon point ($u_0 = 1$).

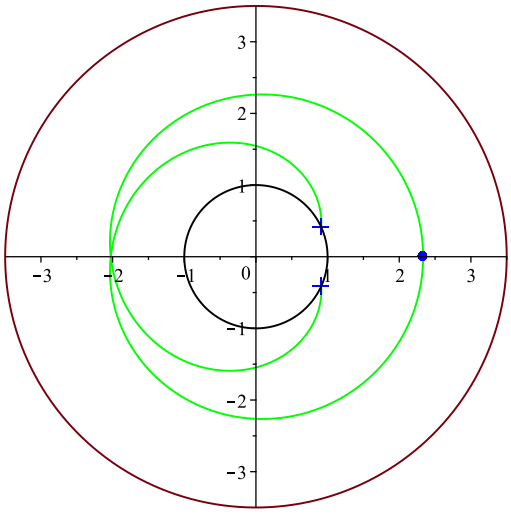

- $u_2 > u_1$

and when we take the plus sign:

- $\frac{8}{9} < \bar{E}^2 < 1$
- $u_1 > u_2$.

4.2.1 $u_2 > u_1$

The double root being greater than the single root gives two classes of orbits. First, there is an asymptotic spiral in from radial value r_1 (or radial infinity) into a circle of radial value r_2. Since $\bar{E}^2 > \frac{8}{9}$ may be greater than 1, the spiral orbit can come from either a finite r_1 or radial infinity. Second, there is an orbit that falls into the singularity by asymptotically spiraling in from r_2. The first integral is given by:

$$\Theta = \phi \pm \frac{2\,\mathrm{sgn}(v\bar{L})}{\sqrt{u_2 - u_1}}\left(\mathrm{arctanh}\sqrt{\frac{u - u_1}{u_2 - u_1}} - \mathrm{arctanh}\sqrt{\frac{u_0 - u_1}{u_2 - u_1}}\right). \tag{4.15}$$

where the plus sign is taken for the asymptotic spiral orbit from r_1 (or infinity) and the minus sign is taken for the orbit that falls in from r_2. For the integral to be well defined, u_0 must either be greater than u_2 (falling in orbit) or between u_1 and u_2 (asymptotic spiral orbit). Of course, if u_1 is negative it becomes an unphysical root

corresponding to a spiral in from radial infinity, u_0 must still be non-negative. For the aysmptotic spiral to r_2, if $u_1 > 0$ we may choose $u_0 = u_1$ so that Θ corresponds to the angular value at the apoapsis where the spiral begins. If the spiral comes in from radial infinity, we can choose our zero-point to be an inertial point $u_0 = u^*$, where $u^* < u_2$ is given by equation (4.3). We cannot take $u_0 = u_2$, as this makes Θ infinite. Also, there is no inertial point u^* such that $u^* > u_2$, so we have no turning or inertial point to choose for u_0 on the falling in orbit, and we choose u_0 to be the horizon point.

4.2.2 $u_1 > u_2$

From the energy ranges above, $\frac{8}{9} < \bar{E}^2 < 1$, so this case only has bound orbits: there is a stable circular orbit at $r_2 = \frac{2M}{u_2}$ and an orbit falling in from $r_1 = \frac{2M}{u_1}$. For the circular orbit the first integral isn't well-defined. For a falling in orbit the first integral is given by:

$$\Theta = \phi + \frac{2\,\mathrm{sgn}(v\bar{L})}{\sqrt{u_1 - u_2}}\left(\arctan\sqrt{\frac{u - u_1}{u_1 - u_2}} - \arctan\sqrt{\frac{u_0 - u_1}{u_1 - u_2}}\right) \tag{4.16}$$

To be well defined, u_0 must be greater than or equal to u_1. We can make the choice $u_0 = u_1$ for our endpoint, so that Θ gives the angular value where the orbit starts to fall in.

4.3 Three Real Roots

The root structure in this case is determined by

$$\Delta > 0. \tag{4.17}$$

If we denote taking the plus sign of (4.12) by $\bar{L}_+^{-2}$ and taking the minus sign by $\bar{L}_-^{-2}$, the above condition on Δ tells us that $\bar{L}^{-2}$ must not take values between $\bar{L}_+^{-2}$ and $\bar{L}_-^{-2}$ for any $\bar{E}$.

The roots are given by

$$u_{3-n} = \frac{1}{3} + \frac{2}{3}\sqrt{1 - 3\bar{L}^{-2}}\cos\Big(\frac{1}{3}\arccos\Big(\frac{(9 - \frac{27}{2}\bar{E}^2)\bar{L}^{-2} + 1}{(1 - 3\bar{L}^{-2})^{\frac{3}{2}}}\Big) - \frac{2\pi n}{3}\Big), \quad n = 0, 1, 2 \tag{4.18}$$

such that $u_1 < u_2 < u_3$.

Figure 4.5: The precessing elliptic orbit in the three real roots case. The periapsis u_2 and apoapsis u_1 points jump in angular value as we move along the orbit. We can choose u_0 to correspond to a turning point (periapsis or apoapsis), or inertial point. For any choice, the first integral will jump depending on which point of the orbit we are on. The choice $u_0 = u_2 = \frac{2M}{r_2}$ is analogous to the Newtonian LRL. We have omitted the orbit of the second kind, whose analysis will be the same as the hyperbolic orbit of the second kind.

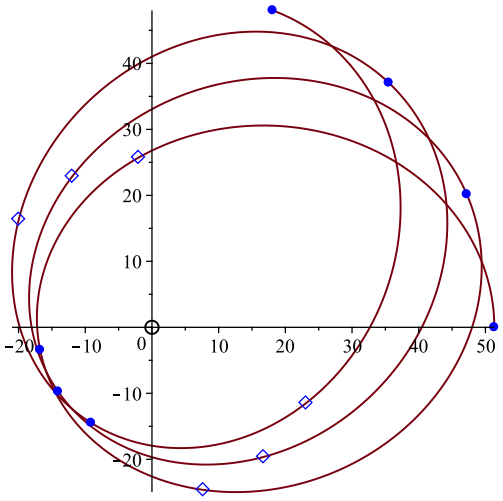

In this case and the next, we express Θ in terms of elliptic integrals:

$$F(\alpha, k) = \int_0^\alpha \frac{d\gamma}{\sqrt{1 - k^2 \sin^2 \gamma}}. \tag{4.19}$$

The first integral is given by

$$\Theta = \phi - \frac{2 \operatorname{sgn}(v\bar{L})}{\sqrt{u_3 - u_1}} (F(\psi(u), k) - F(\psi(u_0), k)) \tag{4.20}$$

where k is defined by

$$k^2 = \frac{u_2 - u_1}{u_3 - u_1} \tag{4.21}$$

and our definition of $\psi(u)$ will depend on whether the orbit is falling in to the singularity or not. We have an orbit that falls in to the singularity for $u \geq u_3$ and a precessing elliptic, parabolic, or hyperbolic orbit when $\max(0, u_1) \leq u \leq u_2$ (precessing elliptic for $u_1 > 0$, parabolic for $u_1 = 0$, and hyperbolic for $u_1 < 0$). For the elliptic, parabolic, or hyperbolic orbit:

$$\psi(u) = \frac{\pi}{2} - \frac{1}{2} \arccos\left(\frac{2u - u_2 - u_1}{u_2 - u_1}\right) \tag{4.22}$$

Figure 4.6: The parabolic orbit in the three real roots case. The periapsis is located at $r_2 = \frac{2M}{u_2}$ (solid dot). The inertial points are marked with diamonds. We can choose u_0 to correspond to the periapsis (u_2) or an inertial point (u^*). The choice $u_0 = u_2 = \frac{2M}{r_2}$ is analogous to the Newtonian LRL. We have omitted the orbit of the second kind, whose analysis will be the same as the hyperbolic orbit of the second kind.

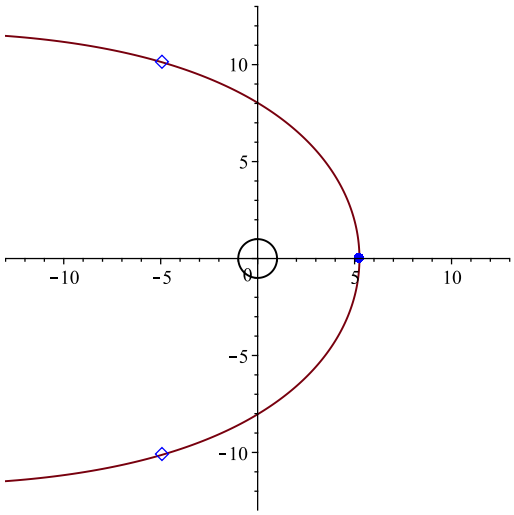

which gives the range $0 \leq \psi(u) \leq \frac{\pi}{2}$ for elliptic orbits or $\left(\frac{\pi}{2} - \frac{1}{2}\arccos\left(\frac{u_2+u_1}{u_1-u_2}\right)\right) < \psi(u) \leq \frac{\pi}{2}$ for hyperbolic or parabolic orbits.

When $u \geq u_3$ the orbit falls in to the singularity and we use:

$$\psi(u) = \arctan\sqrt{\frac{u-u_3}{u_3-u_2}} \tag{4.23}$$

where the range of $\psi(u)$ is again $0 \leq \psi(u) \leq \frac{\pi}{2}$.

In the three real root case, we can choose u_0 to be a turning point. For falling in orbits we take $u_0 = u_3$ so that Θ corresponds to the angular value that the orbit starts falling in from. For parabolic or hyperbolic orbits we take $u_0 = u_2$ so that Θ corresponds to the periapsis angle, in analogy with the Newtonian case where the LRL vector points to the periapsis point.

The elliptic orbits require a special discussion, as they are the only bound Schwarzschild geodesic orbits with more than one turning point. By rearranging (4.4) we get an equation for ϕ along the orbit valid between u_0 and the next turning point. We can piece each of these equations together to get ϕ on the whole orbit. By choosing u_0 to be the periapsis on each piece of the orbit, we get a multi-valued first integral Θ which corresponds to angular value of the periapsis on each part of the orbit. For a more explicit description of the piecewise definition of precessing trajectories with

Figure 4.7: The hyperbolic orbit of the first (left) and second (right) kind in the three real roots case. Unlike the Newtonian hyperbolic orbits, Schwarzschild hyperbolic orbits can wind around the origin some number of times (two windings in this figure).

(a) The periapsis is located at $r_2 = \frac{2M}{u_2}$ (solid dot). The inertial points are marked with diamonds. We can choose u_0 to correspond to the periapsis (u_2) or an inertial point (u^*). The choice $u_0 = u_2 = \frac{2M}{r_2}$ is analogous to the Newtonian LRL.

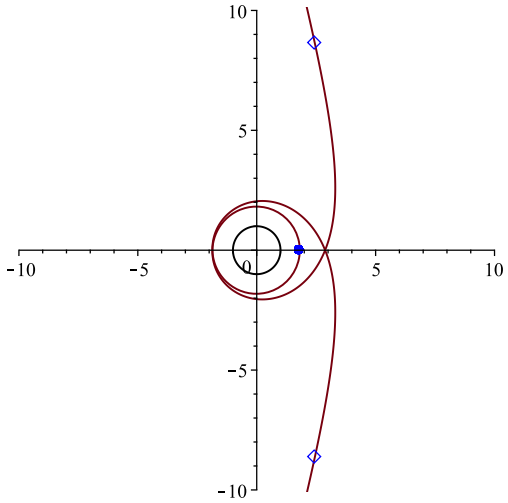

(b) The orbit of the second kind falls into the singularity with an apoapsis at $r_3 = \frac{2M}{u_3}$. We can choose u_0 to correspond to the apoapsis (u_3) or a horizon point (1).

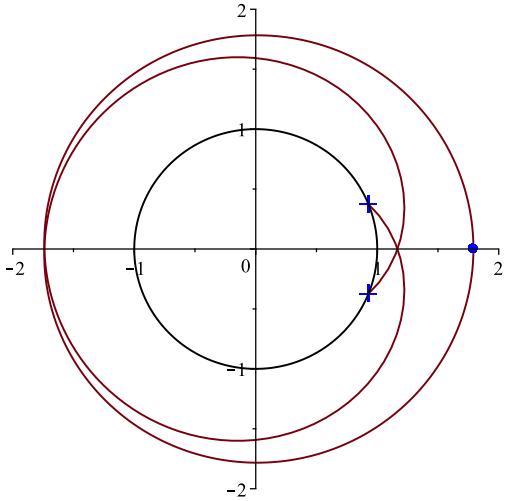

multiple turning points, see [2].

4.4 One Real Root with Two Complex Conjugate Roots

The root structure in this case is determined by

$$\Delta < 0. \tag{4.24}$$

In contrast to the three real roots case (section 4.3), if we denote taking the plus sign in (4.12) by $\bar{L}_+^{-2}$ and the minus sign by $\bar{L}_-^{-2}$, the condition $\Delta < 0$ tells us that $\bar{L}^{-2}$ must be between $\bar{L}_+^{-2}$ and $\bar{L}_-^{-2}$ for any value of $\bar{E}$.

Figure 4.8: Every orbit in the one real root and two complex conjugate roots case falls into the singularity. Bound (left) orbits will have an apoapsis $r_1 = \frac{2M}{u_1}$, and can have zero, one, or two inertial points on either side of the apoapsis. Unbound (right) orbits can have zero, one, or two inertial points total. In this figure, the bound orbit has two inertial points on either side of the apoapsis point, while the unbound orbit has one inertial point total.

(a) We can choose u_0 to correspond to the apoapsis (u_1), an inertial point (u^*), or the horizon point (1).

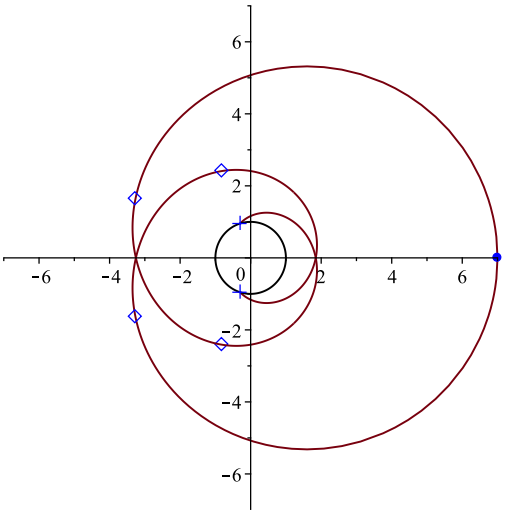

(b) We can choose u_0 to correspond to an inertial point (u^*) or the horizon point (1).

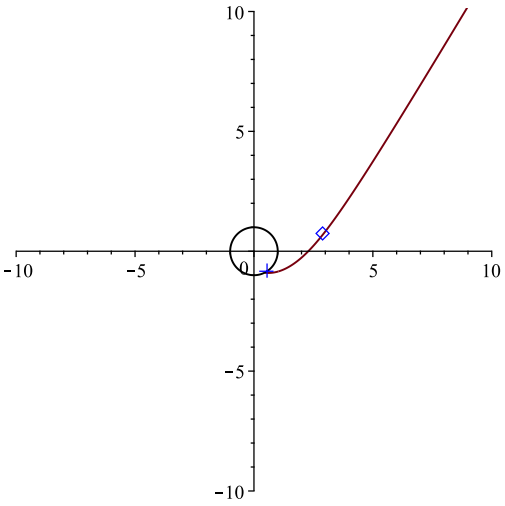

To write the roots, it is convenient to define

$$P = -\left(\frac{1}{6}\left(\left(3\bar{E}^2 - 2\right)\bar{L}^{-2} - \frac{2}{9}\right) - \frac{1}{2}\sqrt{-\frac{\Delta}{27}}\right)^{\frac{1}{3}} \tag{4.25}$$

$$Q = -\left(\frac{1}{6}\left(\left(3\bar{E}^2 - 2\right)\bar{L}^{-2} - \frac{2}{9}\right) + \frac{1}{2}\sqrt{-\frac{\Delta}{27}}\right)^{\frac{1}{3}}. \tag{4.26}$$

The real root is given by

$$u_1 = \frac{1}{3} + P + Q \tag{4.27}$$

and the complex conjugate roots are given by

$$u_2 = \frac{1}{3} + \left(-\frac{1}{2} + i\frac{\sqrt{3}}{2}\right)P + \left(-\frac{1}{2} - i\frac{\sqrt{3}}{2}\right)Q \tag{4.28a}$$

$$u_3 = \frac{1}{3} + \left(-\frac{1}{2} - i\frac{\sqrt{3}}{2}\right)P + \left(-\frac{1}{2} + i\frac{\sqrt{3}}{2}\right)Q. \tag{4.28b}$$

Since u_2 and u_3 are complex conjugates, we have

$$u_2 + u_3 = 2Re(u_2) = \frac{2}{3} - (P + Q) \tag{4.29a}$$

$$(u_2 - u_3)^2 = -(2Im(u_2))^2 = -3(P - Q)^2 \tag{4.29b}$$

so that, although u_2 and u_3 are complex, all expressions in this section contain only the real combinations above. Note also that we can rewrite the right-hand side of (4.29a) as $1 - u_1$, which gives us the identity $u_1 + u_2 + u_3 = 1$.

The first integral is given in terms of the elliptic integral (4.19):

$$\Theta = \phi - \frac{\text{sgn}(v\bar{L})}{\sqrt{\lambda}}(F(\psi(u), k) - F(\psi(u_0), k)) \tag{4.30}$$

where

$$\lambda = \frac{1}{2}\big[(1 - 3u_1)^2 + (u_2 - u_3)^2\big]^{\frac{1}{2}} \tag{4.31}$$

with

$$\psi(u) = \arcsin\left(\left[1 - \frac{2(u_2 - u_3)^2(u - u_1)}{[\lambda + \frac{1}{2}(1 - 3u_1)][(u_2 - u_3)^2 + (2u - (u_2 + u_3))^2]}\right]^{\frac{1}{2}}\right) \tag{4.32}$$

and k is defined by

$$k^2 = \frac{1}{2\lambda}\Big(\lambda + \frac{1}{2}(1 - u_1)\Big). \tag{4.33}$$

In this case, all orbits fall into the singularity from some finite or infinite radial value. For orbits starting from finite radial value, $u \geq u_1$ giving $-\frac{\pi}{2} \leq \psi(u) \leq \frac{\pi}{2}$. For orbits that fall in from infinity the real root becomes non-positive, $u_1 \leq 0$, so $u \geq 0$ and the $\psi(u)$ range becomes

$$\arcsin\left(\left[1 + \frac{2u_1(u_2 - u_3)^2}{[\lambda + \frac{1}{2}(1 - 3u_1)][(u_2 - u_3)^2 + (u_2 + u_3)^2]}\right]^{\frac{1}{2}}\right) \leq \psi(u) \leq \frac{\pi}{2}.$$

For orbits starting from finite radial value, we can choose the turning point $u_0 = u_1$ as our endpoint. In the case of infinite starting point, there is no longer a physical turning point. Because of this, we instead choose an inertial point $u_0 = u^*$ given by equation (4.3) when one exists, or the horizon point when no inertial point exists.

Root Structure		First Kind	Second Kind
Triple Root	zero-point	undefined	horizon point
	trajectory	unstable circular	asymptotic spiral in from unstable circle
Double Root & Single Root, $u_2 > u_1$	zero-point	apoapsis if finite; inertial point otherwise	horizon point
	trajectory	asymptotic spiral in to r_2	asymptotic spiral in from r_2
Double Root & Single Root, $u_1 > u_2$	zero-point	undefined	apoapsis
	trajectory	stable circular	fall in from r_1
Three Real Roots	zero-point	periapsis	apoapsis
	trajectory	precessing elliptic, parabolic, or hyperbolic	fall in from r_3
Single Root & Complex Conjugate Root Pair	zero-point	apoapsis if finite; horizon point otherwise	does not exist
	trajectory	fall in from r_1 or radial infinity	

Table 4.1: A summary of the zero-points and shape of the trajectory for each type of orbit. For falling in and spiraling in orbits, if no final radial value is mentioned, the orbit falls into the singularity at $r = 0$.

4.5 Discussion of Θ

By choosing an appropriate zero-point for each orbit, we were able to find a physically meaningful value for Θ on all non-circular timelike geodesics. These Θ values provide a generalization of the classical Laplace-Runge-Lenz vector from classical mechanics. As noted at the end of chapter 3, the classical LRL vector points from the origin of the Newtonian central potential to the periapsis of a non-circular trajectory. In Schwarzschild spacetime, Θ is generalized so that it corresponds to a larger class of physically meaningful points, including periapsis and apoapsis points, inertial points, and horizon points. This larger class of points is required by the nature of the timelike Schwarzschild geodesics. For example, in the case of a single root with complex conjugate roots, the bound orbit has no periapsis turning point, while the unbound orbit has no turning points at all, making it necessary to choose a different zero-point. Another feature necessitated by the nature of the Schwarzschild geodesics is the multi-valued nature of Θ in the precessing elliptic orbits. This comes from the piecewise definition of the precessing elliptic trajectory. Table 4.1 provides a summary of the physical meaning of the zero-points in each case.

Chapter 5

Conclusions

Figure 5.1: A visualization of the angular jump of Θ on a precessing elliptic orbit. Points on the trajectory (r, ϕ) are connected to (r, Θ) by a dashed circle for three sample points before the apoapsis or by a dotted circle for two additional sample points after the apoapsis. Note that all Θ values before apoapsis correspond to one angular value, and Θ values after apoapsis correspond to another angular value, which has precessed (counter-clockwise in this figure) from the value before apoapsis. The apoapsis is marked with an 'X'.

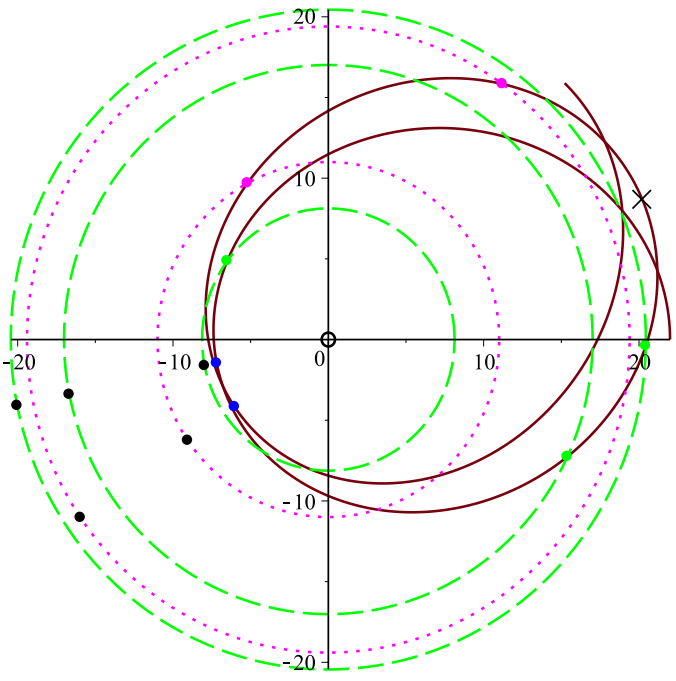

Using the method of characteristics, we derived four first integrals of timelike Schwarzschild geodesics. Two of these first integrals are well known, corresponding to the energy and angular momentum, while the other two are not well known, and

correspond to an angular quantity, Θ, and a temporal quantity, T. By using the freedom to add a constant to a first integral and have it still be a first integral, we were able to set zero-points for our first integrals. In the case of the angular momentum first integral we set our zero-point so that $\hat{L} = 0$ when $\omega = 0$. For the energy, we set the zero-point so that in the Newtonian limit, the first integral reduces to the Newtonian energy per unit mass. For the angular and temporal first integrals, we want to find a zero-point that makes our first integrals physically meaningful, and we do this by choosing a turning point, inertial point, or the horizon point.

By taking the Newtonian limit, we choose the zero-point for both the angular and temporal first integrals to be the turning point at the periapsis of the orbit. By doing this we find that Θ and T correspond to the angle and time of the periapsis point, respectively. For a derivation of Θ and T in central force dynamics, including an explicit derivation for the Kepler problem, see [2]. This corresponds to the classical Laplace-Runge-Lenz vector, which is a vector oriented so that it points from the origin to the periapsis of a non-circular orbit. By choosing a dynamically natural zero-point such as those mentioned above, Θ and T provide a generalization of the LRL vector that we can use in Schwarzschild spacetime.

We find an explicit expression for Θ on each non-circular orbit in Schwarzschild spacetime. Unlike the Newtonian case, we are unable to choose the zero-point to be the periapsis or more generally any turning point on any given orbit, since this may make the expression for Θ singular or complex. Physically, this corresponds to orbits that fall into the singularity at $r = 0$ or asymptote into or away from some radial value. In these cases we use an inertial point as our zero-point, or the horizon point when an inertial point doesn't exist or makes Θ unphysical. Looking at the equation describing the precessing elliptic trajectory given by rearranging equation 4.4:

$$\phi = \Theta - \int_{u_0}^{u} \frac{\operatorname{sgn}(v\bar{L})du}{\sqrt{Q(u)}}, \tag{5.1}$$

defined between the zero-point u_0 and the next turning point, we find that the trajectory is piecewise. Each piece consists of the part of the orbit from u_0 to the next turning point or from a turning point to u_0. Piecing all of these parts together, we get the full precessing orbit. Because of this, Θ will be multi-valued. We choose u_0 to be the periapsis in this case, so that Θ gives the angular value of the periapsis point. Upon crossing an apoapsis, Θ jumps to the angle of the next precessed periapsis. See figure 5.1 for a visualization of this jump.

By choosing the zero-point for any non-circular orbit as described, Θ corresponds

to the angle of a physically meaningful point on the trajectory. Though not evaluated explicitly, the first integral T will correspond to the time of this same point when we choose the zero-point in the same way as Θ. In this way, Θ and T provide a relativistic generalization of the LRL vector on non-circular timelike geodesics in Schwarzschild spacetime.

Bibliography

[1] Milton Abramowitz and Irene A. Stegun. *Handbook of mathematical functions with formulas, graphs, and mathematical tables*. U.S. Dept. of Commerce, National Bureau of Standards, 1972.

[2] Stephen C. Anco, Tyler Meadows, and Vincent Pascuzzi. Some new aspects of first integrals and symmetries for central force dynamics. *Journal of Mathematical Physics*, 57(6):062901, 2016.

[3] Ángel Ballesteros, Alberto Enciso, Francisco J. Herranz, and Orlando Ragnisco. Hamiltonian systems admitting a runge–lenz vector and an optimal extension of bertrand's theorem to curved manifolds. *Communications in Mathematical Physics*, 290(3):1033–1049, Aug 2009.

[4] Dieter R. Brill and Deepak Goel. Light bending and perihelion precession: A unified approach. *American Journal of Physics*, 67(4):316–319, 1999.

[5] Girolamo Cardano and T. Richard Witmer. *The rules of algebra: (Ars magna)*. Dover Publications, 2007.

[6] S. Chandrasekhar. *The Mathematical Theory of Black Holes*. Oxford University Press, 1983.

[7] Charles W. Misner, Kip S. Thorne, and John Archibald Wheeler. *Gravitation*. Princeton University Press, 2017.

[8] A Peres. A classical constant of motion with discontinuities. *Journal of Physics A: Mathematical and General*, 12(10):1711–1713, 1979.

[9] Robert M. Wald. *General relativity*. Univ. of Chicago Press, 2009.